Carrier transport in polycrystalline silicon at high optical injection: transient photoconductance vs. numerical modeling

Uchechi Anyanwu, Christian Harris, Andrey Semichaevsky Department of Chemistry, Physics, and Engineering, Lincoln University, Pennsylvania, 19352, USA

Abstract — This paper discusses our experimental results obtained for several p-type polycrystalline Si wafers using transient photoconductance decay method in combination with a numerical model that accounts for the carrier density dependence of recombination lifetime. Using peak illumination intensities of up to 65 Suns, we are able to estimate the recombination rates for the various carrier recombination mechanisms separately. The model with such realistic recombination parameters produces a realistic diffusion length of minority carriers in Si at high optical injection. Our approach can be applied to the characterization of semiconductor materials for concentrator photovoltaics as well as to design of optoelectronic devices.

Keywords — Silicon, non-radiative recombination, high optical injection, transient photoconductance decay, diffusion-reaction equation.

I. INTRODUCTION

Photovoltaic technologies that reduce the demand for device fabrication and material processing, such as concentrator photovoltaics, have become popular in recent years [1], [2]. Silicon is widely used in solar cell manufacturing, including solar cells that work under concentrated sunlight.

Carrier recombination in Si at room temperature occurs to a large extent due to non-radiative (NR) mechanisms, since the energy bandgap for this material is much larger than the thermal energy, kT at operating temperatures.

Defects in silicon, such as interstitial metal atoms, for instance, Fe and Ti, are known to facilitate charge carrier trapping that can result in the increased non-radiative recombination [1], [2]. When polycrystalline silicon is used to fabricate solar cells, this trap-assisted recombination can reduce the cell fill factors at high optical injection [2], [3].

Previously, carrier density- and irradiance-dependent recombination processes in polycrystalline silicon were studied experimentally [1], [3], [4], [5] and also assessed using computer models of carrier transport [6]. As our previous results [3] may suggest, the shunt resistances found experimentally for some PV cells decrease rapidly as the optical injection increases, which may suggest that some of the recombination processes may involve more than two charge carriers, as in the case of Auger recombination [5].

In this study, we have combined the transient photoconductance (TPC) experiments with computational modeling using experimental carrier lifetimes, in order to explain the recombination processes in polycrystalline silicon at high injection levels.

II. THEORETICAL BACKGROUND

For a semiconductor wafer illuminated by pulsed light, as in TPC, one can describe the carrier transport by a set of diffusion-generation-recombination equations (1a) and (1b) as follows:

$$\frac{\partial n}{\partial t} = G(t) - R(t) + \nabla \cdot \left[-\mu_n n \nabla \Phi + \frac{\mu_n kT}{e} \nabla n \right]$$
 (1a)

$$\frac{\partial p}{\partial t} = G(t) - R(t) - \nabla \cdot [-\mu_p p \nabla \Phi - \frac{\mu_p kT}{\rho} \nabla p], \text{ (1b)}$$

where n and p are electron and hole concentrations, μ_n and μ_p are the electron and hole mobilities, e is the electron charge, Φ is the electric potential, k is the Boltzmann's constant, T is temperature, G(t) and R(t) are the time-dependent electron-hole pair generation and recombination rates, respectively. Recombination rate due to all mechanisms is given by (1c).

$$R = R_{SRH} + R_{rad} + R_{Auger}$$
 (1c)

The carrier recombination rate due to the SRH mechanism at high injection can be approximated as:

$$R_{SRH} = \frac{np}{\tau_{n}p + \tau_{n}n},$$
 (1d)

where τ_n and τ_p are electron and hole lifetimes associated with this carrier recombination mechanism, and the Auger recombination rate for high injection can be assumed to be proportional the third power of injected carrier concentration:

$$R_{Auger} = (C_n n + C_p p) n p, (1e)$$

where C_n and C_p are Auger coefficients for electrons and holes in silicon, respectively.

For our numerical model, the parameters associated with the carrier generation and with SRH (1d) and Auger (1e) recombination can be found experimentally.

For practical purposes, for p-type Si samples, in the absence of applied electric field, equations (1a) and (1b) can be simplified to equation (2) that describes the transport of minority carriers (electrons):

$$\frac{\partial n}{\partial t} = G(t) - \frac{n}{\tau(n)} + \frac{\mu_n kT}{e} \frac{\partial^2 n}{\partial r^2},$$
 (2)

where r is a spatial coordinate.

III. EXPERIMENTAL RESULTS

Two sets of polycrystalline p-type Si wafers were characterized using the WCT-120 carrier lifetime tester from Sinton, Inc. [7]. This instrument is capable of producing optical pulses of up to 65 Suns in intensity and of conducting time-dependent carrier transport measurements. Using the raw data to describe time-dependent irradiance, we have estimated density-dependent minority carrier (electron) lifetimes. Optical pulse FWHM duration was set at 5.5 ms, and a flash lamp with a broad light spectrum that covers the absorption wavelength range of silicon was used. One set of wafers consists of samples that come from the same batch, and the other set has multiple wafers that were made by different companies under different conditions.

Figure 1 shows the experimental carrier lifetime dependences on injected carrier concentrations for a set of three p-type polycrystalline Si wafers that come from the same batch, provided by Solar World, at T=290 K.

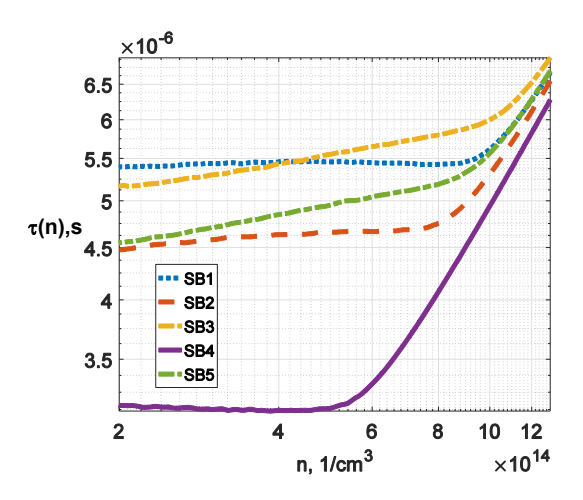


Fig. 1. Electron recombination lifetimes as functions of optically-injected density n, for a set of polycrystalline Si wafers from same batch.

As one can see from Figure 1, the electron lifetime dependences on illumination are very similar among all samples, especially when the electron concentration is around 10^{15} 1/cm³ or higher. Some differences in low-injection lifetime values, e.g., for sample SB4, may be due to specific microstructure or defect density.

Figure 2 presents electron lifetime dependences on the optically-injected carrier density for the set of polycrystalline silicon wafers provided by Sinton, Inc. and taken from multiple batches.

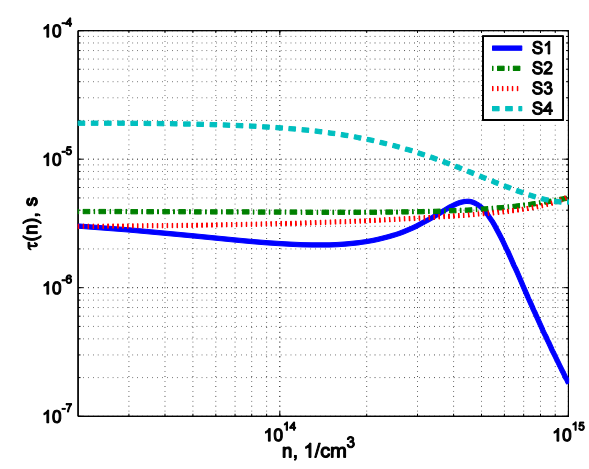


Fig. 2. Electron recombination lifetimes as functions of optically-injected density n, for a set of polycrystalline Si wafers from multiple batches.

As one can see from Figure 2, the electron lifetimes increase slightly with the carrier density and irradiance in samples S2 and S3, while in sample S4, the lifetime decreases (recombination increases). Sample S1, on the other hand exhibits a lifetime dependence with a maximum at $n\approx4.5\times10^{14}$ $1/cm^3$.

IV. NUMERICAL ANALYSIS

Commonly, the carrier lifetime due to all mechanisms of recombination is approximated [1], [2] as:

$$\frac{1}{\tau} = \frac{1}{\tau_{rad}} + \frac{1}{\tau_{SRH}} + \frac{1}{\tau_{Auger}} \approx \frac{1}{\tau_{SRH}} + \frac{1}{\tau_{Auger}},$$
 (3)

where τ_{rad} , τ_{SRH} , and τ_{Auger} are the carrier lifetimes associated with radiative, and non-radiative SRH and Auger recombination mechanisms, respectively. The approximation in (3) holds well due to relatively wide bandgap of Si.

The polynomial fitting for the inverse injection-dependent lifetimes presented in Figures 1, 2 is carried out using equation (4):

$$\frac{1}{\tau(n)} = An^3 + Bn^2 + Cn + D \tag{4}$$

The R² coefficient for the fitting of the inverse lifetime by (4) varied among the samples in the range of 0.96-0.99.

Our numerical calculations are carried out using a simplified version of equation (2), assuming that the generation rate is given by (5):

$$G(t) = \frac{G_{\text{max}}}{\sqrt{2\pi\tau}} e^{\frac{(t-t_0)^2}{2\tau^2}},$$
 (5)

where is G_{max} is the peak generation rate in a pulse, τ is the optical pulse width.

Equation (2) is discretized in accordance with the finitedifference approach, applying Dirichlet boundary conditions for the carrier concentration unmodified by the optical injection at the edges of the 1-D domain. A source condition for the photogeneration rate, in accordance with (5) is applied at r=0. The difference equation (2) is solved in space and in time.

Figure 3 shows how the predicted one-dimensional concentration profile changes with position and time when carriers are optically generated over a small area near r=0. Figure 3a presents the calculation results for an assumed carrier lifetime that approaches infinity, and Figures 3 b,c,d present the carrier density for samples S4, S2, and S3 from Figure 2, respectively.

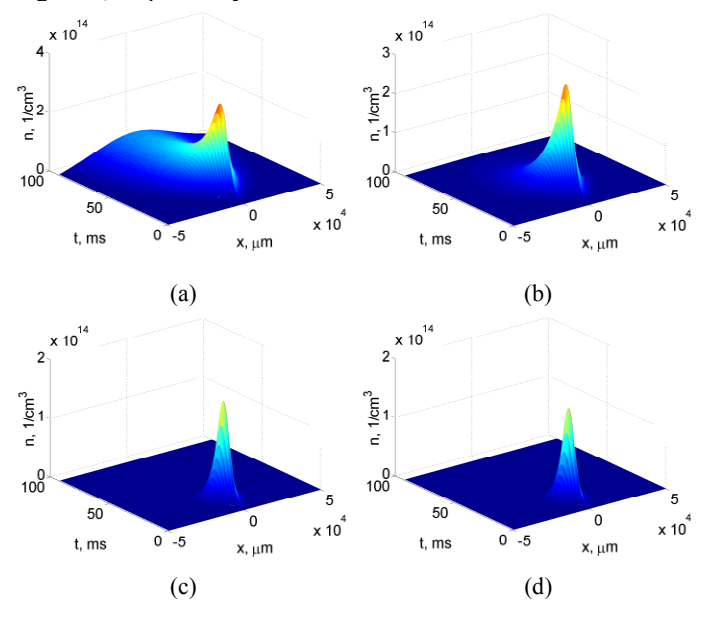


Fig. 3. Electron density in p-type Si samples predicted numerically from (2), a) for $\tau \rightarrow \infty$, b) for $\tau(n)$ of S4, c) for $\tau(n)$ of S2, d) for $\tau(n)$ of S3 from Figure 2.

As one can see from Figures 3a-d, the NR recombination present in the simulations for samples S2 and S3 shown in Figures 3c and 3d greatly reduces the distance that photoexcited electrons travel by diffusion in poly-Si before they recombine. The electrons in sample S4 have longer lifetimes, so the NR recombination has less effect on carrier transport than for samples S2 and S3 with shorter lifetimes. Using the same approach, one can also evaluate the diffusion length dependence on the optical irradiance.

VI. SUMMARY OF THE WORK

In this paper we present and discuss our transient photoconductance measurements at relatively high peak optical intensities for polycrystalline p-type silicon wafers. This is particularly useful for the development and parameterization of a semiclassical carrier transport model that includes realistic lifetime dependences on optical Therefore, one can consider various NR injection. recombination mechanisms, such as Shockley-Reed-Hall and Auger as well as spatial distribution of recombination lifetimes in simulations. The polycrystalline silicon samples that we included in this study show significant variation in minority lifetime dependences on carrier density. However, this variability is much less remarkable when Si samples come from the same fabrication and processing batch. This can suggest that microstructural properties of polycrystalline material strongly affect recombination at high optical injection levels. Results of diffusion length modeling with experimental electron lifetimes included also reveal big differences in spatiotemporal carrier concentrations among various poly-Si samples.

VII. ACKNOWLEDGEMENT

This work was supported through the NSF-RIA award HRD-1505377.

REFERENCES

- [1] D. McDonald, Sinton, R.A., Cuevas A., "Recombination in highly injected silicon," *Journal of Applied Physics*, vol. 89, pp. 2772-2777, 2001.
- [2] D. Macdonald and Cuevas A., "Reduced fill factors in multicrystalline silicon solar cells due to injection-level dependent bulk recombination lifetimes," *Progress in Photovoltaics: Research and Applications*, vol. 8, pp. 363-375, 2000
- [3] E. Connell, Semichaevsky, A., "Degradation of polycrystalline Si solar cell efficiency with increased incident optical power – experiments and theory," 43rd IEEE PVSC, Portland, OR, 2016.
- [4] J. Schmidt, "Temperature- and injection-dependent lifetime spectroscopy for the characterization of defect centers in semiconductors," *Appl. Phys. Lett.*, vol. 82, pp. 2178, 2003.
- [5] Pang S.K., A. W. Smith, A. Rohatgi, "Effect of trap location and trap-assisted Auger recombination on silicon solar cell performance," *IEEE Trans. on Electron Devices*, vol. 42, pp. 662-668, 2002.
- [6] S. K. Saha, A.M. Farhan, S. I. Reba, et al., "An analytical model of dark saturation current of silicon solar cell considering both SRH and Auger recombination," *IEEE Regional Symposium on Micro- and Nanoelectronics (RSM)*, Malaysia, 2011.
- [7] Sinton, Inc., "WCT-120 lifetime tester manual", 2016.